View metadata, citation and similar papers at core.ac.uk

brought to you by CORE

provided by Elsevier - Publisher Connector

Computers and Mathematics with Applications 63 (2012) 943–956

Contents lists available at SciVerse ScienceDirect

Computers and Mathematics with Applications

journal homepage: www.elsevier.com/locate/camwa

A Petrov–Galerkin method for solving the generalized regularized long wave (GRLW) equation

Thoudam Roshan *

Department of Mathematics, Manipur University, Canchipur 795003, Imphal, India

ARTICLE INFO

Article history:
Received 7 January 2011
Received in revised form 30 November 2011
Accepted 30 November 2011

Keywords:
Petrov–Galerkin
Product approximation
Quintic *B*-spline
Solitary waves
Solitons

ABSTRACT

The generalized regularized long wave (GRLW) equation is solved numerically by the Petrov–Galerkin method which uses a linear hat function as the trial function and a quintic *B*-spline function as the test function. Product approximation has been used in this method. A linear stability analysis of the scheme shows it to be conditionally stable. Test problems including the single soliton and the interaction of solitons are used to validate the suggested method, which is found to be accurate and efficient. Finally, the Maxwellian initial condition pulse is studied.

© 2011 Elsevier Ltd. All rights reserved.

1. Introduction

The regularized long wave (RLW) equation given by

$$u_t + u_x + \delta\, uu_x - \mu\, u_{xxt} = 0, \tag{1}$$

where δ and μ are positive constants and the subscripts x and t denote space and time derivatives respectively is a model nonlinear partial differential equation used for the simulation of one-dimensional nonlinear waves propagating in dispersive media. Peregrine [1] was the first to derive this equation for modeling the development of an undular bore. Later on, Benjamin et al. [2] proposed the use of the RLW equation as an alternative preferable to the more classical Korteweg–de Vries (KdV) equation, for modeling a larger class of physical phenomena. The solutions of this equation are kinds of solitary waves known as solitons whose shapes are not affected by collision. The RLW equation was solved numerically by various methods such as Galerkin [3–6], least squares [7] and collocation methods [8,9]. Indeed, the RLW equation is a special case of the generalized regularized long wave (GRLW) equation given by

$$u_t + u_x + p(p+1)u^p u_x - \mu\, u_{xxt} = 0, \tag{2}$$

where p is a positive integer. The GRLW equation was studied by applying the finite difference method for a Cauchy Problem [10] and by the Adomian decomposition method [11,12]. Another special case of the GRLW equation is the modified regularized long wave (MRLW) equation with $p = 2$. Comparatively little work has been done for this case. Some of these cases are found in [13,14]. In this work, the Petrov–Galerkin method is developed for the GRLW equation, using a linear hat function as the trial function and a quintic *B*-spline function as the test function. Here the proposed method is shown to represent accurately the migration of single solitary waves for the cases $p = 2$, 3 and 4. Interaction of solitary waves and other properties are also studied.

* Tel.: +91 0385 2435125; fax: +91 0385 2435831.
E-mail address: roshandmc@gmail.com.

0898-1221/$ – see front matter © 2011 Elsevier Ltd. All rights reserved.
doi:10.1016/j.camwa.2011.11.059

2. Petrov–Galerkin method

For convenience GRLW equation (2) is rewritten as

$$u_t + u_x + p\left(u^{p+1}\right)_x - \mu\, u_{xxt} = 0. \tag{3}$$

Dirichlet boundary conditions on the region $a \le x \le b$ are assumed in the form $u(a,t) = u(b,t) = 0$. The form of the initial pulse will be chosen so that at large distances from the pulse $|u|$ is extremely small and essentially attains a free space boundary condition $u = 0$. The space interval $a \le x \le b$ is discretized with $N+1$ uniform grid points $x_j = a + jh$, where $j = 0, 1, 2, \ldots, N$ and the grid spacing is given by $h = (b-a)/N$. Let $U_j(t)$ denote the approximate solution to the exact solution $u(x_j, t)$. Following the method used in [15] for solving the KdV equation by the Petrov–Galerkin method, we modify the method in order to solve Eq. (3). Using the Petrov–Galerkin method, we assume that the approximate solution of Eq. (3) is

$$u_h(x,t) = \sum_{j=0}^{N} U_j(t)\phi_j(x). \tag{4}$$

The product approximation technique [16] is used for treating the nonlinear term in the following manner:

$$u_h^{p+1}(x,t) = \sum_{j=0}^{N} U_j^{p+1}(t)\phi_j(x) \tag{5}$$

where $\phi_j(x),\ j = 0, 1, 2, \ldots, N$ are the usual piecewise linear "hat" functions given by

$$\phi_j(x) = \begin{cases} 1 + (x - jh)/h, & x \in [x_{j-1}, x_j] \\ 1 - (x - jh)/h, & x \in [x_j, x_{j+1}] \\ 0, & \text{otherwise.} \end{cases}$$

The unknown functions $U_j(t),\ j = 0, 1, 2, \ldots, N$ are determined from the variational formulation

$$\left((u_h)_t, \psi_j\right) + \left((u_h)_x, \psi_j\right) + p\left((u_h^{p+1})_x, \psi_j\right) - \mu\left((u_h)_{xxt}, \psi_j\right) = 0 \tag{6}$$

where $\psi_j(x),\ j = 0, 1, 2, \ldots, N$ are test function, which are taken to be the quintic B-splines given by

$$\psi_j(x) = \frac{1}{h^5}\begin{cases} \left(x - x_{j-3}\right)^5, & [x_{j-3}, x_{j-2}] \\ \left(x - x_{j-3}\right)^5 - 6\left(x - x_{j-2}\right)^5, & [x_{j-2}, x_{j-1}] \\ \left(x - x_{j-3}\right)^5 - 6\left(x - x_{j-2}\right)^5 + 15\left(x - x_{j-1}\right)^5, & [x_{j-1}, x_j] \\ \left(x - x_{j-3}\right)^5 - 6\left(x - x_{j-2}\right)^5 + 15\left(x - x_{j-1}\right)^5 - 20\left(x - x_j\right)^5, & [x_j, x_{j+1}] \\ \left(x - x_{j-3}\right)^5 - 6\left(x - x_{j-2}\right)^5 + 15\left(x - x_{j-1}\right)^5 - 20\left(x - x_j\right)^5 + 15\left(x - x_{j+1}\right)^5, & [x_{j+1}, x_{j+2}] \\ \left(x - x_{j-3}\right)^5 - 6\left(x - x_{j-2}\right)^5 + 15\left(x - x_{j-1}\right)^5 - 20\left(x - x_j\right)^5 + 15\left(x - x_{j+1}\right)^5 - 6\left(x - x_{j+2}\right)^5, & \\ \quad [x_{j+2}, x_{j+3}] & \\ 0, \quad \text{otherwise} & \end{cases}$$

and $(,)$ denotes the usual inner product $(f, g) = \int_a^b f(x)g(x)dx$.

Integrating by parts and using the fact that $\psi(a) = \psi(b) = 0$, Eq. (6) leads to the formulation

$$\left((u_h)_t, \psi_j\right) + \left((u_h)_x, \psi_j\right) + p\left((u_h^{p+1})_x, \psi_j\right) + \mu\left((u_h)_{xt}, (\psi_j)_x\right) = 0. \tag{7}$$

Each linear hat function covers two elements so that each element $[x_j, x_{j+1}]$ is covered by two linear hat functions. On the other hand each quintic B-spline covers six elements so that each element $[x_j, x_{j+1}]$ is covered by six splines. In terms of locale co-ordinate system given by

$$\xi = x - x_j, \quad 0 \le \xi \le h \tag{8}$$

both the linear hat functions, ϕ_j and the quintic B-spline functions, ψ_j over the element $[x_j, x_{j+1}]$ can be defined as follows:

$$\left.\begin{array}{l} \phi_j = \xi/h \\ \phi_{j+1} = 1 - \xi/h \end{array}\right\} \tag{9}$$

and

$$\left.\begin{aligned}
\psi_{j-2} &= 1 - 5\frac{\xi}{h} + 10\left(\frac{\xi}{h}\right)^2 - 10\left(\frac{\xi}{h}\right)^3 + 5\left(\frac{\xi}{h}\right)^4 - \left(\frac{\xi}{h}\right)^5\\
\psi_{j-1} &= 26 - 50\frac{\xi}{h} + 20\left(\frac{\xi}{h}\right)^2 + 20\left(\frac{\xi}{h}\right)^3 - 20\left(\frac{\xi}{h}\right)^4 + 5\left(\frac{\xi}{h}\right)^5\\
\psi_{j} &= 66 - 60\left(\frac{\xi}{h}\right)^2 + 30\left(\frac{\xi}{h}\right)^4 - 10\left(\frac{\xi}{h}\right)^5\\
\psi_{j+1} &= 26 - 50\frac{\xi}{h} + 20\left(\frac{\xi}{h}\right)^2 - 20\left(\frac{\xi}{h}\right)^3 - 20\left(\frac{\xi}{h}\right)^4 + 10\left(\frac{\xi}{h}\right)^5\\
\psi_{j+2} &= 1 + 5\frac{\xi}{h} + 10\left(\frac{\xi}{h}\right)^2 + 10\left(\frac{\xi}{h}\right)^3 + 5\left(\frac{\xi}{h}\right)^4 - 5\left(\frac{\xi}{h}\right)^5\\
\psi_{j+3} &= \left(\frac{\xi}{h}\right)^5
\end{aligned}\right\}. \tag{10}$$

Thus, over the typical element $[x_{j-1}, x_j]$ each inner product involved in Eq. (7) can be evaluated as follows:

$$\begin{aligned}
\left((u_h)_t, \psi_j\right) &= \dot{U}_{j-3}\int_0^h \phi_{j-3}(x)\psi_{j-3}(x)dx + \dot{U}_{j-2}\int_0^h \phi_{j-2}(x)\psi_{j-3}(x)dx\\
&\quad + \dot{U}_{j-2}\int_0^h \phi_{j-2}(x)\psi_{j-2}(x)dx + \dot{U}_{j-1}\int_0^h \phi_{j-1}(x)\psi_{j-2}(x)dx\\
&\quad + \dot{U}_{j-1}\int_0^h \phi_{j-1}(x)\psi_{j-1}(x)dx + \dot{U}_{j}\int_0^h \phi_{j}(x)\psi_{j-1}(x)dx\\
&\quad + \dot{U}_{j}\int_0^h \phi_{j}(x)\psi_{j}(x)dx + \dot{U}_{j+1}\int_0^h \phi_{j+1}(x)\psi_{j}(x)dx\\
&\quad + \dot{U}_{j+1}\int_0^h \phi_{j+1}(x)\psi_{j+1}(x)dx + \dot{U}_{j+2}\int_0^h \phi_{j+2}(x)\psi_{j+1}(x)dx\\
&\quad + \dot{U}_{j+2}\int_0^h \phi_{j+2}(x)\psi_{j+2}(x)dx + \dot{U}_{j+3}\int_0^h \phi_{j+3}(x)\psi_{j+2}(x)dx\\
&= \frac{h}{42}\left(\dot{U}_{j-3} + 120\dot{U}_{j-2} + 1191\dot{U}_{j-1} + 2416\dot{U}_j + 1191\dot{U}_{j+1} + 120\dot{U}_{j+2} + \dot{U}_{j+3}\right).
\end{aligned}$$

Similarly,

$$\begin{aligned}
\left((u_h)_x, \psi_j\right) &= \frac{1}{6}\left(-U_{j-3} - 56U_{j-2} - 245U_{j-1} + 245U_{j+1} + 56U_{j+2} + U_{j+3}\right), \left((u_h^{p+1})_x, \psi_j\right)\\
&= \frac{1}{6}\left(-(U_{j-3})^{p+1} - 56(U_{j-2})^{p+1} - 245(U_{j-1})^{p+1} + 245(U_{j+1})^{p+1} + 56(U_{j+2})^{p+1} + (U_{j+3})^{p+1}\right)
\end{aligned}$$

and $\left((u_h)_{xt}, (\psi_j)_x\right) = \frac{1}{h}\left(-\dot{U}_{j-3} - 24\dot{U}_{j-2} - 15\dot{U}_{j-1} + 80\dot{U}_j - 15\dot{U}_{j+1} - 24\dot{U}_{j+2} - \dot{U}_{j+3}\right)$.

Putting all these values of the inner products in Eq. (7) and simplifying, we get the following system of ordinary differential equations (ODEs):

$$\left.\begin{aligned}
&\alpha\dot{U}_{j-3} + \beta\dot{U}_{j-2} + \gamma\dot{U}_{j-1} + \delta\dot{U}_j + \gamma\dot{U}_{j+1} + \beta\dot{U}_{j+2} + \alpha\dot{U}_{j+3}\\
&= \frac{1}{6h}\left[U_{j-3} + 56U_{j-2} + 245U_{j-1} - 245U_{j+1} - 56U_{j+2} - U_{j+3}\right]\\
&+ \frac{p}{6h}\left[(U_{j-3})^{p+1} + 56(U_{j-2})^{p+1} + 245(U_{j-1})^{p+1} - 245(U_{j+1})^{p+1} - 56(U_{j+2})^{p+1} - (U_{j+3})^{p+1}\right]
\end{aligned}\right\} \tag{11}$$

where $\alpha = 1/42 - \mu/h^2$, $\beta = 120/42 - 24\mu/h^2$, $\gamma = 1191/42 - 15\mu/h^2$, $\delta = 2416/42 + 80\mu/h^2$ and "$\dot{}$" denote differentiation with respect to, t.

Now to solve the ODEs, we assume U_j^n to be a fully discrete approximation to the exact solution $u(x_j, t_n)$, where $t_n = n\Delta t$ and Δt is the time step size. Using the central difference scheme for the time derivative, $\dot{U} = \frac{U^{n+1} - U^{n-1}}{2\Delta t}$, Eq. (11) is reduced

to the system of equations

$$\left.\begin{aligned}&\alpha U_{j-3}^{n+1}+\beta U_{j-2}^{b+1}+\gamma U_{j-1}^{n+1}+\delta U_j^{n+1}+\gamma U_{j+1}^{n+1}+\beta U_{j+2}^{n+1}+\alpha U_{j+3}^{n+1}\\&\quad=\alpha U_{j-3}^{n-1}+\beta U_{j-2}^{n-1}+\gamma U_{j-1}^{n-1}+\delta U_j^{n-1}+\gamma U_{j+1}^{n-1}+\beta U_{j+2}^{n-1}+\alpha U_{j+3}^{n-1}\\&\qquad+\frac{\Delta t}{3h}\left[U_{j-3}^{n}+56U_{j-2}^{n}+245U_{j-1}^{n}-245U_{j+1}^{n}-56U_{j+2}^{n}-U_{j+3}^{n}\right]\\&\qquad+\frac{p\Delta t}{3h}\left[(U_{j-3}^{n})^{p+1}+56(U_{j-2}^{n})^{p+1}+245(U_{j-1}^{n})^{p+1}-245(U_{j+1}^{n})^{p+1}-56(U_{j+2}^{n})^{p+1}-(U_{j+3}^{n})^{p+1}\right]\end{aligned}\right\}\tag{12}$$

where $j=3,4,\ldots,N-3$ and $U_0=U_1=U_2=0=U_{N-2}=U_{N-1}=U_N$.

The system (12) is three time level scheme, so we require two initial time levels and in our practical calculations, the exact values at time equals zero and time equals Δt are used for the required initial conditions. However, in general the exact solution at time Δt is not known. In such cases, we use a two level scheme. For this scheme, we replace the time derivative $\dot{U}$ by the forward difference approximation $\dot{U}=\left(U^{n+1}-U^{n}\right)/\Delta t$ and the parameter U by the Crank–Nicolson formulation $U=\left(U^{n+1}+U^{n}\right)/2$, then the system of ODEs (11) reduce to a system of nonlinear equations

$$\left.\begin{aligned}&\alpha U_{j-3}^{n+1}+\beta U_{j-2}^{n+1}+\gamma U_{j-1}^{n+1}+\delta U_j^{n+1}+\gamma U_{j+1}^{n+1}+\beta U_{j+2}^{n+1}+\alpha U_{j+3}^{n+1}\\&\qquad-\frac{\Delta t}{12h}\left[U_{j-3}^{n+1}+56U_{j-2}^{n+1}+245U_{j-1}^{n+1}-245U_{j+1}^{n+1}-56U_{j+2}^{n+1}-U_{j+3}^{n+1}\right]\\&\qquad-\frac{p\Delta t}{12h}\left[(U_{j-3}^{n+1})^{p+1}+56(U_{j-2}^{n+1})^{p+1}+245(U_{j-1}^{n+1})^{p+1}-245(U_{j+1}^{n+1})^{p+1}-56(U_{j+2}^{n+1})^{p+1}-(U_{j+3}^{n+1})^{p+1}\right]\\&\quad=\alpha U_{j-3}^{n}+\beta U_{j-2}^{n}+\gamma U_{j-1}^{n}+\delta U_j^{n}+\gamma U_{j+1}^{n}+\beta U_{j+2}^{n}+\alpha U_{j+3}^{n}\\&\qquad+\frac{\Delta t}{12h}\left[U_{j-3}^{n}+56U_{j-2}^{n}+245U_{j-1}^{n}-245U_{j+1}^{n}-56U_{j+2}^{n}-U_{j+3}^{n}\right]\\&\qquad+\frac{p\Delta t}{12h}\left[(U_{j-3}^{n})^{p+1}+56(U_{j-2}^{n})^{p+1}+245(U_{j-1}^{n})^{p+1}-245(U_{j+1}^{n})^{p+1}-56(U_{j+2}^{n})^{p+1}-(U_{j+3}^{n})^{p+1}\right]\end{aligned}\right\}.\tag{13}$$

Using the initial condition at time $t=0$, the system of Eq. (13) is solved by Newtons method to get the solution at time $t=\Delta t$. Then the system of linear equations (12) is used to get the solutions at the successive time steps. The matrices of the system (12) are septadiagonal and are solved with a variant of the Thomas algorithm [17].

3. Stability analysis

To investigate the stability of the scheme Eq. (12) we apply the Von Neumann stability analysis. Assuming u in the nonlinear term $u^p u_x$ of the GRLW equation (2) as locally constant $\tilde{u}$, the linearized scheme is

$$\left.\begin{aligned}&\alpha U_{j-3}^{n+1}+\beta U_{j-2}^{b+1}+\gamma U_{j-1}^{n+1}+\delta U_j^{n+1}+\gamma U_{j+1}^{n+1}+\beta U_{j+2}^{n+1}+\alpha U_{j+3}^{n+1}\\&\quad=\alpha U_{j-3}^{n-1}+\beta U_{j-2}^{n-1}+\gamma U_{j-1}^{n-1}+\delta U_j^{n-1}+\gamma U_{j+1}^{n-1}+\beta U_{j+2}^{n-1}+\alpha U_{j+3}^{n-1}\\&\qquad+\frac{(1+p(p+1)\tilde{u}^p)\Delta t}{3h}\left[U_{j-3}^{n}+56U_{j-2}^{n}+245U_{j-1}^{n}-245U_{m+1}^{n}-56U_{j+2}^{n}-U_{j+3}^{n}\right]\end{aligned}\right\}.\tag{14}$$

Substituting the Fourier mode

$$U_j^n=\xi^n e^{ij\theta},\quad \theta=hk \text{ and } i=\sqrt{-1}\tag{15}$$

where k is the mode number and h is the space step size into the system of Eq. (14), we obtain

$$\xi^{n+1}=g\xi^n\tag{16}$$

where the growth factor, g, is determined by

$$g^2+2ig\sin\eta-1=0\tag{17}$$

$$\text{and }\sin\eta=\frac{(1+p(p+1)\tilde{u}^p)\Delta t}{3h}\,\frac{\sin3\theta+56\sin2\theta+256\sin\theta}{2\alpha\cos3\theta+2\beta\cos2\theta+2\gamma\cos\theta+\delta}.\tag{18}$$

The roots of Eq. (17) are

$$g_1=-e^{i\eta},\qquad g_2=e^{-i\eta}.\tag{19}$$

Thus for stability the roots must both have modulus less than or equal to 1. Therefore, η must be real. From Eq. (18) we have

$$\left|\frac{(1+p(p+1)\tilde{u}^p)\Delta t}{3h}\,\frac{\sin3\theta+56\sin2\theta+256\sin\theta}{2\alpha\cos3\theta+2\beta\cos2\theta+2\gamma\cos\theta+\delta}\right|\le1$$

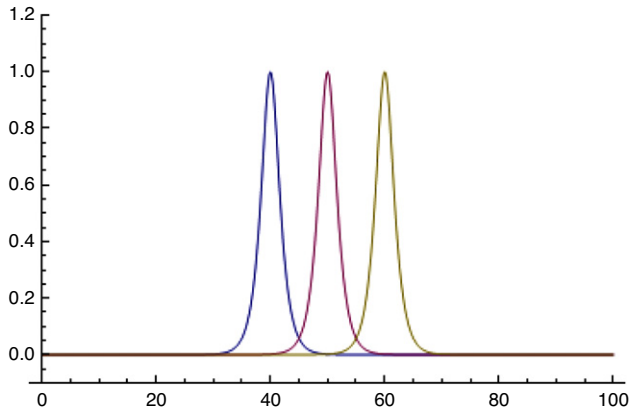

Fig. 1. Single solitary wave with $p = 2$, $c = 1$, $x_0 = 40$, $0 \le x \le 100$ at level time $t = 0, 5, 10$.

and this gives, the following condition:

$$\Delta t < \frac{360h}{323(1 + p(p+1)\tilde{u}^p)}. \tag{20}$$

Since, $\tilde{u}$ is locally the maximum wave amplitude, usually unity, therefore for any problem of practical significance, it is possible to chose the time step Δt to satisfy the condition (20).

4. Numerical applications

The exact solution of the GRLW equation is found [14,18] to be

$$u(x,t) = \sqrt[p]{\frac{c(p+2)}{2p}\,\mathrm{sec}\,h^2\left[\frac{p}{2}\sqrt{\frac{c}{\mu(c+1)}}(x - (c+1)t - x_0)\right]} \tag{21}$$

where x_0 is an arbitrary constant and the GRLW equation has three invariants of motion given in [14,18]

$$I_1 = \int_a^b u dx, \qquad I_2 = \int_a^b \left(u^2 + \mu(u_x)^2\right) dx, \qquad I_3 = \int_a^b \left(u^4 - \mu(u_x)^2\right) dx. \tag{22}$$

The L_2 and L_∞ error norms are used to measure the accuracy of the present scheme and to compare our result with both exact values, Eq. (21) as well as other results in the literature whenever available.

4.1. Single solitary wave

First we take $p = 2$. The analytic values of the conservation laws as given in Eq. (22) are [14]:

$$I_1 = \frac{\pi\sqrt{c}}{q}, \qquad I_2 = \frac{2c}{q} + \frac{2\mu qc}{3}, \qquad I_3 = \frac{4c^2}{3q} - \frac{2\mu qc}{3} \tag{23}$$

where $q = \sqrt{\frac{c}{\mu(1+c)}}$.

In this case two sets of parameters have been chosen and considered for our computational work. The first set is chosen to be $c = 1$, $h = 0.2$, $\Delta t = 0.025$, $\mu = 1$ and $x_0 = 40$ with range [0, 100] to coincide with the collocation methods of [13,14]. Thus, the solitary wave has amplitude 1.0 and the simulations are done up to $t = 10$. Values of the three invariants as well as L_2 and L_∞-error norms from our method have been computed and reported in Table 1. Analytical values of the invariants are $I_1 = 4.442883$, $I_2 = 3.299832$ and $I_3 = 1.414214$. The changes of the invariants $I_1 \times 10^4$, $I_2 \times 10^4$ and $I_3 \times 10^4$ from their initial values are less than 0.2, 0.5 and 0.41, respectively. Error deviations are changed in the range of $-1.34468 \times 10^{-3} <$ error $< 1.68740 \times 10^{-3}$. Fig. 1 illustrates the motion of the single solitary wave for this case at different time levels. The second set is chosen to be $c = 0.3$, $h = 0.1$, $\Delta t = 0.01$, $\mu = 1$ and $x_0 = 40$ with range [0, 100]; then the amplitude is 0.54772. The simulations are done up to $t = 20$. Table 2 represent values of the three invariants and error norms from the given method in this case. Analytical values of the invariants are $I_1 = 3.581967$, $I_2 = 1.345077$ and $I_3 = 0.153723$. The changed of the invariants $I_1 \times 10^5$, $I_2 \times 10^5$ and $I_3 \times 10^5$ from their initial values are less than 0.1, 0.1 and 0.2 respectively i.e. approach zero throughout, indicating the efficiency of the present scheme. The error deviations are changed in the ranges of $-2.38044 \times 10^{-5} <$ error $< 3.01923 \times 10^{-5}$.

Table 1
Invariants and error norms for single solitary wave: $p = 2$, amplitude $= 1$, $c = 1$, $\Delta t = 0.025$, $h = 0.2$, $\mu = 1$, $0 \le x \le 100$.

t	I_1	I_2	I_3	$L_2 \times 10^3$	$L_\infty \times 10^3$
0	4.44288	3.29980	1.41416	0.0	0.0
1	4.44288	3.29980	1.41416	0.55741	0.44389
2	4.44288	3.29980	1.41416	0.97773	0.65459
3	4.44288	3.29979	1.41417	1.29239	0.79807
4	4.44288	3.29980	1.41416	1.56154	0.92933
5	4.44289	3.29987	1.41418	1.81166	1.05631
6	4.44288	3.29980	1.41416	2.05367	1.18322
7	4.44288	3.29979	1.41417	2.29236	1.30957
8	4.44288	3.29980	1.41416	2.52992	1.43566
9	4.44289	3.29979	1.41417	2.76741	1.56161
10	4.44288	3.29981	1.41416	3.00533	1.68749

Table 2
Invariants and error norms for single solitary wave: $p = 2$, amplitude $= 0.54772$, $c = 0.3$, $\Delta t = 0.01$, $h = 0.1$, $\mu = 1$, $0 \le x \le 100$.

t	I_1	I_2	I_3	$L_2 \times 10^4$	$L_\infty \times 10^4$
0	3.58197	1.34508	0.153722	0.0	0.0
2	3.58197	1.34508	0.153724	0.105264	0.069574
4	3.58197	1.34508	0.153723	0.192827	0.113714
6	3.58197	1.34508	0.153723	0.264867	0.144165
8	3.58197	1.34508	0.153723	0.328089	0.170207
10	3.58197	1.34508	0.153723	0.386081	0.193911
12	3.58197	1.34508	0.153722	0.440843	0.216419
14	3.58197	1.34508	0.153723	0.493586	0.238258
16	3.58197	1.34508	0.153723	0.544969	0.259698
18	3.58197	1.34508	0.153723	0.595425	0.280889
20	3.58197	1.34508	0.153723	0.645295	0.301923

Table 3
Comparisons of results for single solitary wave of MRLW equation with $h = 0.2$, $\Delta t = 0.025$, $\mu = 1$, $0 \le x \le 100$.

Schemes	I_1	I_2	I_3	$L_2 \times 10^3$	$L_\infty \times 10^3$
Analytic	4.44288	3.29983	1.41421	0.	0.
Our scheme	4.44288	3.29981	1.41416	3.00533	1.68749
Cubic B-spline collocation [13]	4.44288	3.29983	1.41420	9.30196	5.43718
Cubic B-spline coll-CN [14]	4.442	3.299	1.413	16.39	9.24
Cubic B-spline coll + PA-CN [14]	4.440	3.296	1.411	20.3	11.2

Table 4
Invariants and error norms for single solitary wave: $p = 3$, amplitude $= 1$, $c = 6/5$, $\Delta t = 0.025$, $h = 0.1$, $\mu = 1$, $0 \le x \le 100$.

t	I_1	I_2	I_3	$L_2 \times 10^3$	$L_\infty \times 10^3$
0	3.79713	2.88119	0.972913	0.0	0.0
1	3.79713	2.88127	0.972558	1.28555	1.06172
2	3.79713	2.88122	0.972388	2.13434	1.47042
3	3.79713	2.88124	0.972331	2.85711	1.86885
4	3.79713	2.88121	0.972324	3.55504	2.26771
5	3.79713	2.88124	0.972280	4.24994	2.66795
6	3.79713	2.88123	0.972282	4.94712	3.07151
7	3.79713	2.88123	0.972280	5.64770	3.48026
8	3.79713	2.88125	0.972272	6.35159	3.88952
9	3.79713	2.88121	0.972295	7.05835	4.29906
10	3.79713	2.88123	0.972243	7.76745	4.70875

Comparisons with our results with exact solution as well as the recorded values in [13,14] have been made and tabulated in Table 3 at $t = 10$. The parameters used in the present paper are the same as those used in the cited paper. The superiority of the present method over the previous ones is clear.

Secondly, we take $p = 3$. In this case also two sets of parameters have been chosen and considered. First, we take $c = 1.2$, $h = 0.1$, $\Delta t = 0.025$, $\mu = 1$ and $x_0 = 40$ with range [0, 100]. Thus the solitary wave has amplitude 1.0 and the simulations are done up to $t = 10$. Table 4 represent values of the three invariants and error norms. The changes of the invariants $I_1 \times 10^4$, $I_2 \times 10^4$ and $I_3 \times 10^4$ from their initial values are less than 0.01, 0.7 and 6.8 respectively. Error deviations are changed in the range of $-4.06499 \times 10^{-3} < \text{error} < 4.70875 \times 10^{-3}$. Fig. 2 illustrates the motion of the single solitary wave for this case at different time levels. The second set of parameters are $c = 0.3$, $h = 0.1$, $\Delta t = 0.01$, $\mu = 1$ and $x_0 = 40$ with range [0, 100]. Thus the solitary wave has amplitude 0.6 and the simulations are done up to $t = 10$. The computed

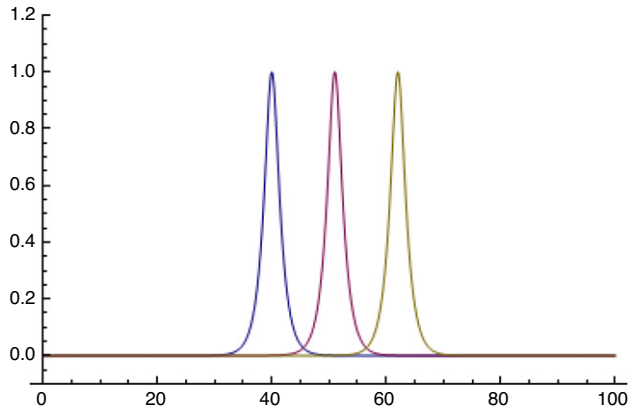

Fig. 2. Single solitary wave with $p = 3$, $c = 1.2$, $x_0 = 40$, $0 \le x \le 100$ at level time $t = 0, 5, 10$.

Table 5
Invariants and error norms for single solitary wave: $p = 3$, amplitude $= 0.6$, $\Delta t = 0.01$, $h = 0.1$, $\mu = 1$, $0 \le x \le 100$.

t	I_1	I_2	I_3	$L_2 \times 10^4$	$L_\infty \times 10^4$
0	3.67755	1.56574	0.226837	0.0	0.0
1	3.67755	1.56574	0.226839	0.10196	0.080060
2	3.67755	1.56574	0.226838	0.19402	0.140623
3	3.67755	1.56574	0.226836	0.27291	0.177988
4	3.67755	1.56574	0.226838	0.34368	0.209309
5	3.67755	1.56574	0.226838	0.40991	0.238594
6	3.67755	1.56574	0.226835	0.47366	0.266636
7	3.67755	1.56574	0.226839	0.53601	0.294588
8	3.67755	1.56574	0.226837	0.59759	0.322149
9	3.67755	1.56574	0.226835	0.65876	0.349668
10	3.67755	1.56574	0.226837	0.71976	0.377228

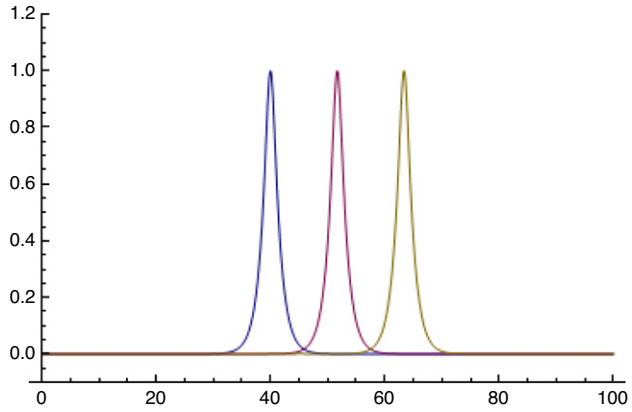

Fig. 3. Single solitary wave with $p = 4$, $c = 4/3$, $x_0 = 40$, $0 \le x \le 100$ at level time $t = 0, 5, 10$.

value of the three invariants and the error norms are reported in Table 5. The changes of the invariants $I_1 \times 10^5$, $I_2 \times 10^5$ and $I_3 \times 10^5$ from their initial values are less than 0.1, 0.1 and 0.3 respectively i.e. approach zero throughout. Error deviations are changed in the range $-2.9127 \times 10^{-5} <$ error $< 3.77228 \times 10^{-5}$.

Finally, we take $p = 4$, and two sets of parameters are chosen and considered. First set of parameters are $c = 4/3$, $h = 0.1$, $\Delta t = 0.01$, $\mu = 1$ and $x_0 = 40$ with range [0, 100]. Thus the solitary wave has amplitude 1.0 and the simulation are done up to $t = 10$. The motion of a single solitary wave using the above scheme corresponding to the above set of parameters has been computed and reported in Table 6. Fig. 3 represents the motion of a single solitary wave at different time levels. The changes of the invariants $I_1 \times 10^3$, $I_2 \times 10^3$ and $I_3 \times 10^3$ from their initial values are less than 0.02, 0.12 and 0.31 respectively. Error deviations are changed in the range $-1.40836 \times 10^{-3} <$ error $< 1.5662 \times 10^{-3}$. In the second set, we consider the following parameters $c = 0.3$, $h = 0.1$, $\Delta t = 0.01$, $\mu = 1$ and $x_0 = 40$ with range [0, 100]. The amplitude of the solitary wave in this case is 0.6 and the simulation are done up to $t = 10$. The computed values of the three invariants and the error

Table 6
Invariants and error norms for single solitary wave: $p = 4$, amplitude $= 1$, $c = 4/3$, $\Delta t = 0.025$, $h = 0.1$, $\mu = 1$, $0 \le x \le 100$.

t	I_1	I_2	I_3	$L_2 \times 10^3$	$L_\infty \times 10^3$
0	3.46865	2.67163	0.729173	0.0	0.0
1	3.46866	2.67167	0.728987	0.35156	0.28704
2	3.46866	2.67165	0.728938	0.59123	0.42042
3	3.46865	2.67160	0.729005	0.81964	0.55849
4	3.46866	2.67174	0.728872	1.04951	0.70021
5	3.46866	2.67165	0.728931	1.28158	0.84282
6	3.46866	2.67171	0.728864	1.51540	0.98686
7	3.46866	2.67156	0.729056	1.75052	1.13205
8	3.46866	2.67166	0.728915	1.98658	1.27432
9	3.46866	2.67166	0.728948	2.22336	1.42247
10	3.46866	2.67168	0.728881	2.46065	1.56620

Table 7
Invariants and error norms for single solitary wave: $p = 4$, amplitude $= 0.6$, $c = 0.3$, $\Delta t = 0.01$, $h = 0.1$, $\mu = 1$, $0 \le x \le 100$.

t	I_1	I_2	I_3	$L_2 \times 10^4$	$L_\infty \times 10^4$
0	3.75923	1.72999	0.289407	0.0	0.0
1	3.75923	1.72999	0.289410	0.15887	0.13864
2	3.75923	1.73000	0.289405	0.29690	0.22193
3	3.75923	1.73000	0.289405	0.41666	0.27662
4	3.75923	1.73000	0.289406	0.53011	0.32955
5	3.75923	1.72999	0.289403	0.54225	0.38257
6	3.75923	1.72999	0.289403	0.75515	0.43636
7	3.75923	1.73000	0.289406	0.86966	0.49116
8	3.75923	1.73000	0.289405	0.98615	0.54704
9	3.75923	1.72999	0.289403	1.10472	0.60402
10	3.75923	1.72999	0.289406	1.22539	0.66207

norms are recorded in Table 7. The changes of the invariants $I_1 \times 10^4$, $I_2 \times 10^4$ and $I_3 \times 10^4$ from their initial values are less than 0.01, 0.2 and 0.05 respectively. Error deviations are changed in the range of $-0.539702 \times 10^{-4} <$ error $< 0.662066 \times 10^{-4}$. In all the cases, we find decreasing the values of h and Δt to 0.1 and 0.01 respectively, the results are more accurate as it is clear from the Tables.

4.2. Interaction of two GRLW solitary waves

Here we study the interaction of two well separated solitary waves having different amplitudes and traveling in the same direction. The initial condition is given by

$$u(x, 0) = \sum_{i=1}^{2} \sqrt[p]{\frac{c_i(p+2)}{2p}\, \mathrm{sec}\, h^2 \left[\frac{p}{2}\sqrt{\frac{c_i}{\mu(c_i+1)}}\,(x - x_i)\right]} \tag{24}$$

where c_i and x_i, $i = 1, 2$ are arbitrary constants. In this case also we take $p = 2$, 3 and 4 respectively. For $p = 2$, the analytic values of the conservation laws are [14]

$$I_1 = \sum_{i=1}^{2} \frac{\pi\sqrt{c_i}}{q_i}, \qquad I_2 = \sum_{i=1}^{2} \left(\frac{2c_i}{q_i} + \frac{2\mu q_i c_i}{3}\right), \qquad I_3 = \sum_{i=1}^{2} \left(\frac{4c_i^2}{3q_i} - \frac{2\mu q_i c_i}{3}\right) \tag{25}$$

where $q_i = \sqrt{\frac{c_i}{\mu(1+c_i)}}$. For computational work we choose, $c_1 = 4, c_2 = 1, x_1 = 25, x_2 = 55, h = 0.2, \Delta t = 0.025$ and $\mu = 1$ with interval $[0, 250]$. The amplitudes are in the ratio 2:1. The analytical values of the invariants are $I_1 = 11.467698$, $I_2 = 14.629243$ and $I_3 = 22.880466$. Numerical values of the three invariants have been computed and reported in Table 8. The simulations are done up to $t = 20$. Changes of the invariants $I_1 \times 10^2$, $I_2 \times 10^2$ and $I_3 \times 10^2$ from their initial values are less than 0.25, 0.58 and 0.25 respectively. Fig. 4(a)–(d) show the computer plot of the interaction of two solitary waves at different time levels.

For $p = 3$, we choose the following parameters $c_1 = 48/5, c_2 = 6/5, x_1 = 20, x_2 = 50, h = 0.1, \Delta t = 0.01$ and $\mu = 1$ with interval $[0, 120]$. The amplitudes of the two solitary waves are in the ratio $2 : 1$. The simulations are done up to $t = 6$. The interaction of two solitary waves in this case are shown in Fig. 5(a)–(d). For $p = 4$ we take $c_1 = 64/3, c_2 = 4/3, x_1 = 20, x_2 = 80, h = 0.125, \Delta t = 0.01$ and $\mu = 1$ with interval $[0, 200]$, so that the amplitudes of the two solitary waves are in the ratio $2 : 1$. In this case also the simulations are done up to $t = 6$. The computed values of the two invariants of motion for the cases $p = 3$ and $p = 4$ are recorded in Table 9. For the case $p = 3$, the changes of the

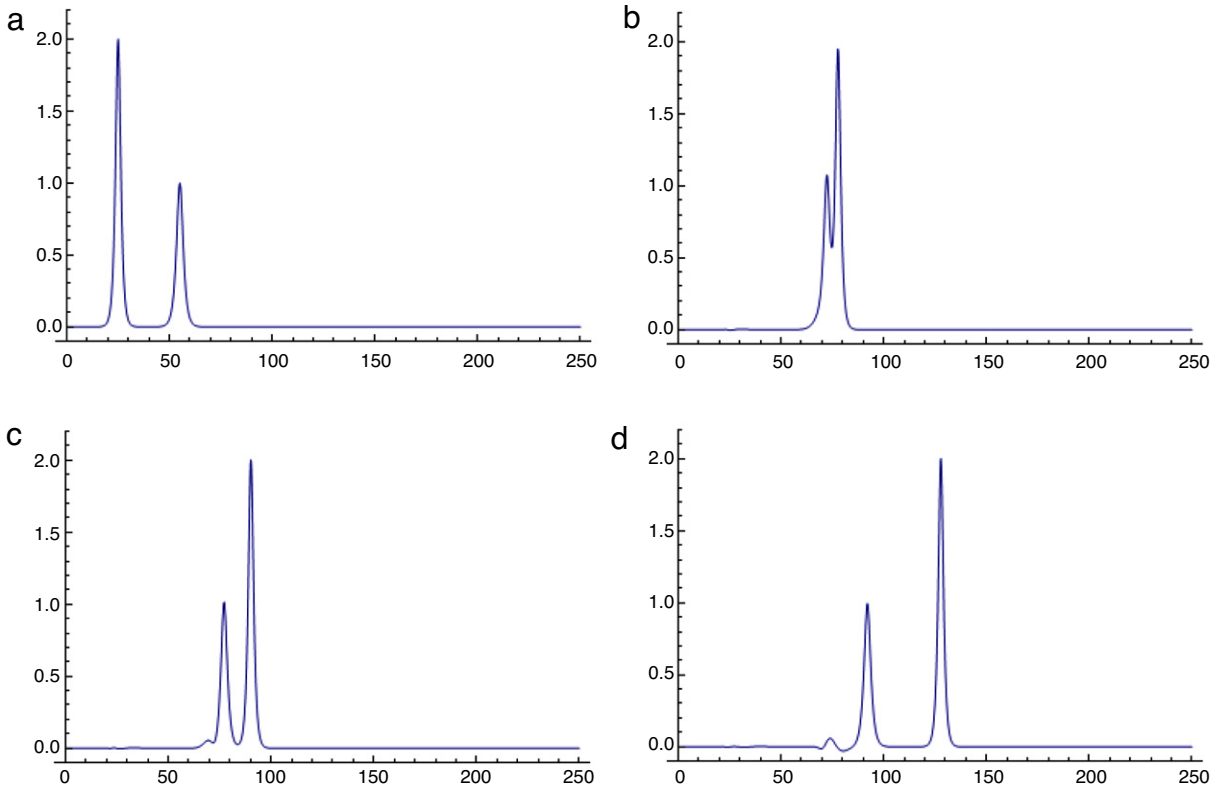

Fig. 4. $p = 2$: interaction of two solitary waves at (a) $t = 0$ (b) $t = 10$ (c) $t = 10.5$ (d) $t = 20$.

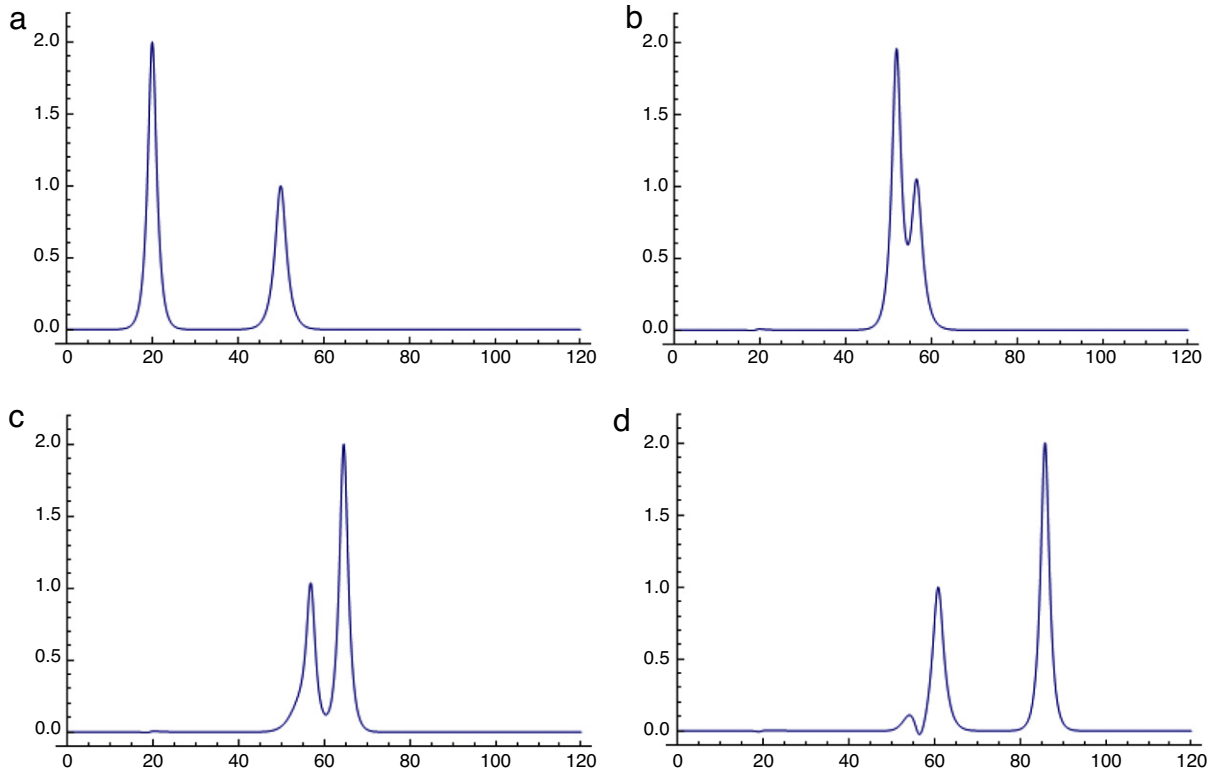

Fig. 5. $p = 3$: interaction of two solitary waves at (a) $t = 0$ (b) $t = 3$ (c) $t = 5$ (d) $t = 6$.

Table 8
Invariants for interaction of two solitary waves with $p = 2$, $c_1 = 4$, $c_2 = 1$, $x_1 = 25$, $x_2 = 55$, $h = 0.2$, $\Delta t = 0.025$, $\mu = 1$, $0 \le x \le 250$.

t	I_1	I_2	I_3
0	11.4677	14.6286	22.8788
2	11.4677	14.6299	22.8799
4	11.4677	14.6292	22.8811
6	11.4677	14.6285	22.8812
8	11.4677	14.6229	22.8798
10	11.4677	14.6235	22.8789
12	11.4677	14.6299	22.8803
14	11.4677	14.6288	22.8812
16	11.4677	14.6295	22.8805
18	11.4677	14.6296	22.8807
20	11.4677	14.6299	22.8806

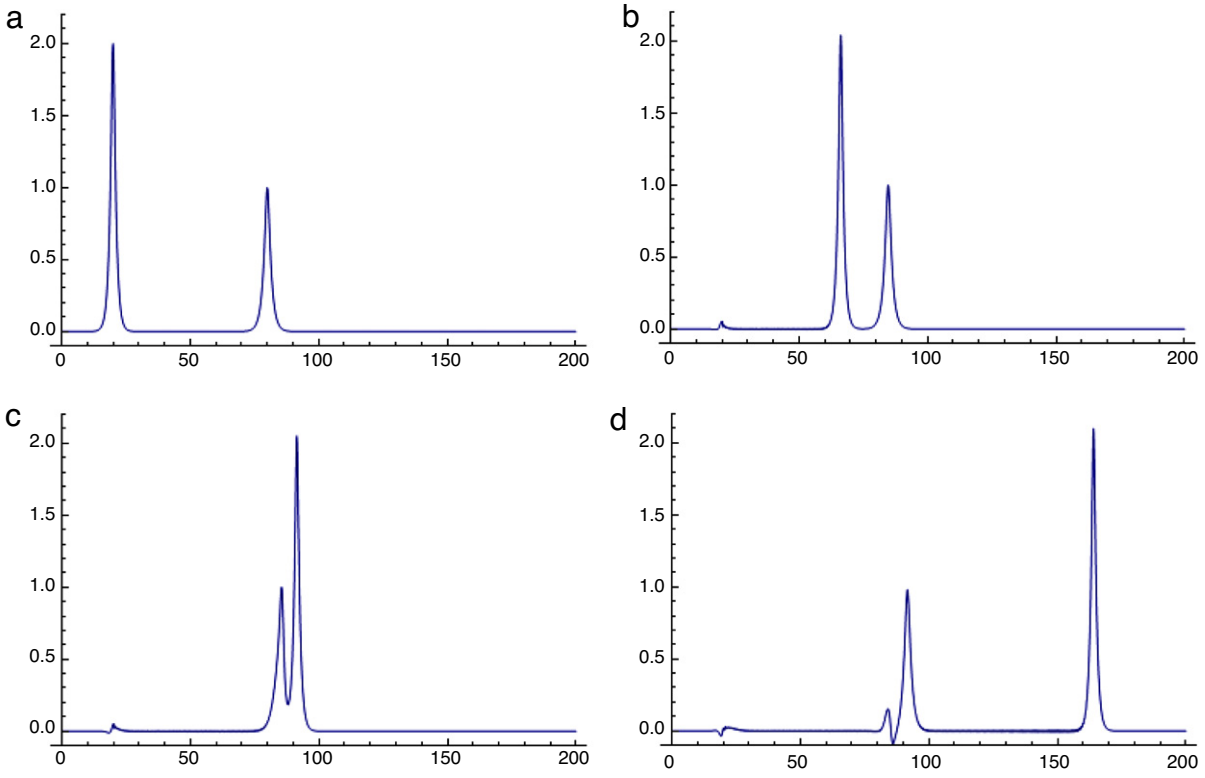

Fig. 6. $p = 4$: interaction of two solitary waves at (a) $t = 0$ (b) $t = 2$ (c) $t = 3$ (d) $t = 6$.

Table 9
Invariants for interaction of two solitary waves with $p = 3$ and $p = 4$.

t	$p = 3$			$p = 4$		
	I_1	I_2	I_3	I_1	I_2	I_3
0	9.69075	12.9444	17.0184	8.83427	12.1697	14.0302
1	9.69074	12.9459	16.9819	8.83427	12.3179	13.8420
2	9.69074	12.9452	16.9835	8.84204	12.3700	13.9607
3	9.69074	12.9379	17.0591	8.84205	12.4530	14.0887
4	9.69074	12.9453	16.9261	8.84209	12.5703	13.9805
5	9.69074	12.9457	16.8781	8.83421	12.6304	14.2357
6	9.69074	12.9454	16.9113	8.83434	12.6103	14.6974

invariants $I_1 \times 10^4$, $I_2 \times 10^2$ and I_3 from their initial values are less than 0.2, 0.66 and 0.15 respectively and the changes of the invariants $I_1 \times 10^3$, I_2 and I_3 for the case $p = 4$ are less than 0.24,0.4407 and 0.67 respectively. Fig. 6(a)–(d) show the interaction of two solitary waves at different time levels for the case $p = 4$.

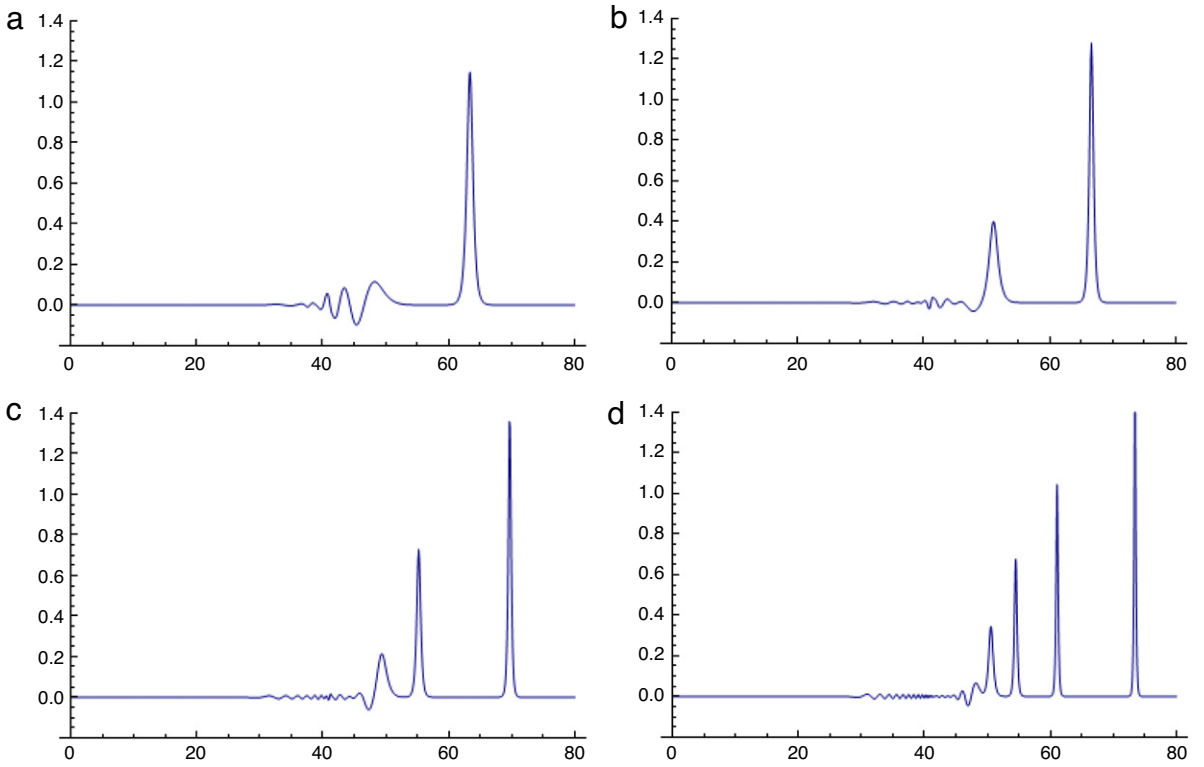

Fig. 7. Maxwellian initial condition $p = 2$: with (a) at $t = 10$, $\mu = 0.1$ (b) at $t = 10$, $\mu = 0.05$ (c) at $t = 10$, $\mu = 0.025$ (d) at $t = 10$, $\mu = 0.01$.

4.3. Maxwellian initial condition

In this section, evolution of a train of solitary waves of the GRLW equation has been studied by using the Maxwellian initial condition

$$u(x, 0) = \mathrm{Exp}\left(-(x - 20)^2\right) \tag{26}$$

for various values of μ. As it is known that the Maxwellian initial condition, the behavior of the solution depends on the value of μ [10,11]. For $\mu \gg \mu_c$ where μ_c is some critical value, the Maxwellian initial condition does not break up into solitons but exhibits rapidly oscillating wave packets. When $\mu = \mu_c$ a mixed type of solution is found, which consists of a leading soliton and an oscillating tail. For $\mu < \mu_c$, the Maxwellian breaks up into a number of solitons according to the values of μ. We take $\mu = 0.1, 0.05, 0.025$ and 0.01 for all values of p. For the case $p = 2$, the computed values of the invariants of motion for different values of μ are recorded in Table 10. In this case the computer plot of the breaking of solitons are shown in Fig. 7(a)–(d). Similarly, for $p = 3$ the breaking of solitons from Maxwellian are shown in Fig. 8(a)–(d). Finally, for $p = 4$ the breaking of solitons are shown in Fig. 9(a)–(d). For the case $p = 2$, the simulation is done up to $t = 10$. For this case the changes of the invariants I_1, I_2 and I_3 from their initial values are less than 0.00012, 0.018 and 0.02 respectively. Similarly, for the case $p = 3$ the changes of the invariants I_1, I_2 and I_3 from their initial values are less than 0.0005, 0.014 and 0.242 respectively. Lastly, the changes of the invariants I_1, I_2 and I_3 from their initial values are less than 0.04, 0.18 and 0.493 respectively, for the case $p = 4$. The computed values of the invariants I_1, I_2 and I_3 for the cases $p = 3$ and $p = 4$ are recorded in Table 11.

5. Conclusion

The Petrov–Galerkin method using the linear hat function and quintic B-spline function as trial and test functions respectively has been successfully implemented to study the solitary waves of the GRLW equation. It has been shown that our scheme is conditionally stable and it is more accurate than any other method available in the literature. We have tested our scheme using single solitary waves for which the analytic solution is known and then extend this scheme to the study of the interaction of two solitary waves as well as Maxwellian initial condition where no analytic solution is known. It has also been observed that the conservation laws are reasonably well satisfied for the interaction of two solitary waves as well as Maxwellian initial condition.

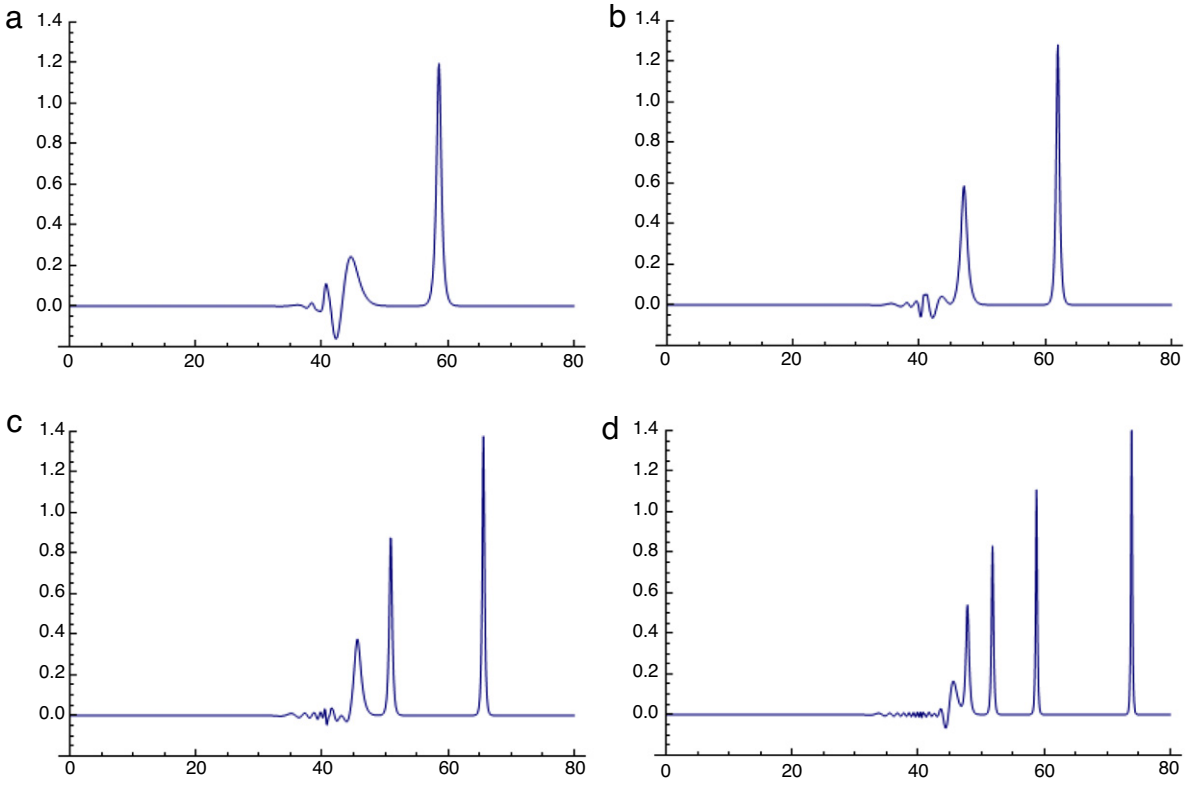

Fig. 8. Maxwellian initial condition $p = 3$: with (a) at $t = 6$, $\mu = 0.1$ (b) at $t = 6$, $\mu = 0.05$ (c) at $t = 6$, $\mu = 0.025$ (d) at $t = 6$, $\mu = 0.01$.

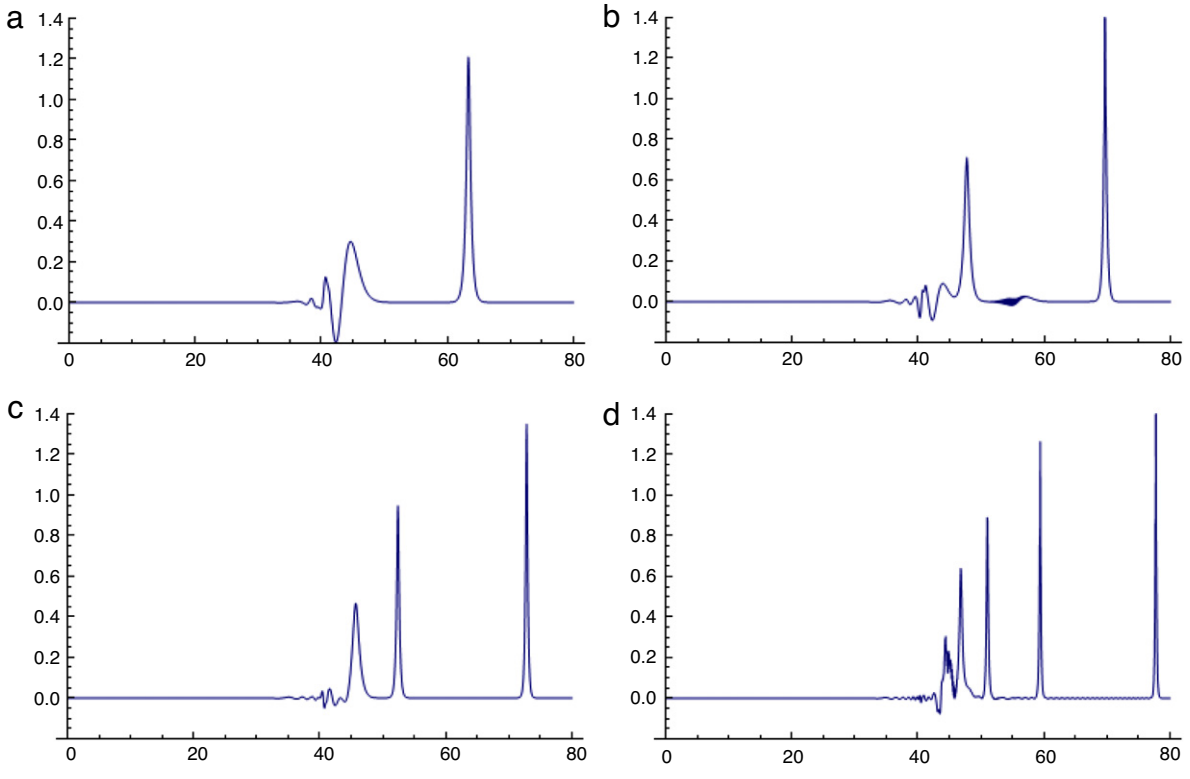

Fig. 9. Maxwellian initial condition $p = 4$: with (a) at $t = 6$, $\mu = 0.1$ (b) at $t = 6$, $\mu = 0.05$ (c) at $t = 6$, $\mu = 0.025$ (d) at $t = 6$, $\mu = 0.01$.

Table 10
Invariants of GRLW equation using the Maxwellian initial condition with $p = 2$.

μ	t	I_1	I_2	I_3
0.1	0	1.77245	1.3786	0.7609
	2	1.77245	1.3786	0.7609
	4	1.77245	1.3786	0.7609
	6	1.77245	1.3809	0.7619
	8	1.77246	1.3811	0.7616
	10	1.77245	1.3808	0.7618
0.05	0	1.77245	1.31596	0.823546
	2	1.77245	1.31952	0.825965
	4	1.77243	1.31881	0.826471
	6	1.77239	1.31951	0.825686
	8	1.77246	1.31898	0.825787
	10	1.77246	1.31898	0.825787
0.025	0	1.77245	1.28463	0.854868
	2	1.77247	1.29066	0.858833
	4	1.77242	1.28959	0.857314
	6	1.77238	1.29011	0.854909
	8	1.77229	1.29109	0.858933
	10	1.77245	1.28935	0.863683
0.01	0	1.77245	1.26585	0.873692
	2	1.77249	1.28261	0.892944
	4	1.77254	1.28355	0.892696
	6	1.77249	1.28315	0.892359
	8	1.77243	1.28274	0.891287
	10	1.77256	1.28345	0.891335

Table 11
Invariants of GRLW equation using the Maxwellian initial condition with $p = 3$ and 4.

μ	t	$p = 3$			$p = 4$		
		I_1	I_2	I_3	I_1	I_2	I_3
0.1	0	1.77245	1.37860	0.76090	1.77245	1.37864	0.760895
	2	1.77246	1.38153	0.60423	1.77245	1.38781	0.459452
	4	1.77245	1.38333	0.60085	1.77246	1.38739	0.452817
	6	1.77245	1.38433	0.59908	1.77245	1.38945	0.449163
0.05	0	1.77245	1.31596	0.82354	1.77245	1.31596	0.823546
	2	1.77248	1.32567	0.62306	1.77241	1.33735	0.484501
	4	1.77248	1.32331	0.62437	1.77222	1.34989	0.482068
	6	1.77248	1.32394	0.62472	1.77212	1.45168	0.489711
0.025	0	1.77245	1.28464	0.85489	1.77245	1.28464	0.854893
	2	1.77241	1.30674	0.63669	1.77250	1.29488	0.484544
	4	1.77255	1.30795	0.63615	1.77244	1.29413	0.478627
	6	1.77235	1.30806	0.63579	1.77249	1.29626	0.479621
0.01	0	1.77245	1.26585	0.87369	1.77245	1.26585	0.873692
	2	1.77205	1.27959	0.63522	1.77152	1.34049	0.419430
	4	1.77219	1.27782	0.63199	1.76994	1.43090	0.389015
	6	1.77245	1.27627	0.63288	1.75648	1.40577	0.381194

Acknowledgments

The author acknowlege Dr. K.S. Bhamra for extending his inspirations in this work and also offer sincere thanks to the refree for giving valuable comments and suggestions.

References

[1] D.H. Peregrine, Calculations of the development of an undular bore, J. Fluid Mech. 25 (2) (1966) 321–330.
[2] T.B. Benjamin, J.L. Bona, J.J. Mahony, Model equations for long waves in non-linear dispersive systems, Philos. Trans. R. Soc. Lond. Ser. A 272 (1972) 47–78.
[3] M.E. Alexander, J.L. Morris, Galerkin method applied to some model equation for nonlinear dispersive waves, J. Comput. Phys. 30 (1979) 428–451.
[4] I. Dag, Least squares quadratic *B*-spline finite element method for regularized long wave equation, Comput. Methods Appl. Mech. Eng. 182 (2000) 205–215.
[5] L.R.T. Gardner, G.A. Gardner, İ Dağ, A *B*-spline finite element method for the regularized long wave equation, Commun. Numer. Methods Eng. 11 (1995) 59–68.
[6] İ Dağ, B. Saka, D. Irk, Galerkin method for the numerical solution of the RLW equation using quintic *B*-splines, J. Comput. Appl. Math. 190 (2006) 532–547.
[7] L.R.T. Gardner, G.A. Gardner, A. Doğan, A least squares finite element scheme for the RLW equation, Commun. Numer. Methods Eng. 12 (1996) 795–804.

[8] I. Dag, B. Saka, G. Irk, Application of cubic *B*-splines for numerical solution of RLW equation, Appl. Math. Comput. 159 (2004) 373–389.
[9] A.A. Soliman, M.H. Hussein, Collocation solution for RLW equation with septic spline, J. Appl. Math. Comput. 161 (2005) 623–636.
[10] L. Zhang, A finite difference scheme for generalized regularized long-wave equation, Appl. Math. Comput. 168 (2005) 962–972.
[11] D. Kaya, A numerical simulation of solitary-wave solutions of the generalized regularized long wave equation, Appl. Math. Comput. 149 (2004) 833–841.
[12] D. Kaya, El. Syed, An application of the decomposition method for the generalized KdV and RLW equation, Chaos Solitons Fractals 17 (2003) 869–877.
[13] A.K. Khalifa, K.T. Raslan, H.M. Alzubaidi, A collocation method with cubic *B*-splines for solving the MRLW equation, Comput. Appl. Math. 212 (2008) 406–418.
[14] L.R.T. Gardner, G.A. Gardner, F.A. Ayoub, N.K. Amein, Approximations of solitary waves of the MRLW equation by *B*-spline finite element, Arab. J. Sci. Eng. 22 (1997) 183–193.
[15] J.M. Sanz-Serna, I. Christie, Petrov–Galerkin methods for nonlinear dispersive waves, J. Comput. Phys. 39 (1993) 94–102.
[16] I. Christie, D.F. Griffths, A.R. Mitchell, J.M. Sanz-Serna, Product approximations for nonlinear problems in finite element methods, IMA J. Numer. Anal. 1 (1981) 253–266.
[17] S.I. Zaki, Solitary waves of the Korteweg–de Vries-Burgers' equation, Comput. Phys. Commun. 126 (2000) 207–218.
[18] Anjan Biswas, Solitary waves for power-law regularized long-wave equation and $R(m, n)$ equation, Nonlinear Dyn. 59 (2010) 423–446.